

# Integration of photodetectors with lasers for optical interconnects using 200 mm wafer scale III-V/SOI technology

Thijs Spuesens<sup>1</sup>, Liu Liu<sup>1,2</sup>, Diedrik Vermeulen<sup>1</sup>, Jing Zhao<sup>3</sup>, Pedro Rojo Romeo<sup>4</sup>, Philippe Regreny<sup>4</sup>, Laurent Grenouillet<sup>5</sup>, Jean-Marc Fédeli<sup>5</sup>, Dries Van Thourhout<sup>1</sup>

*1. Photonics research group, INTEC department, Ghent University-IMEC, St-Pietersnieuwstraat 41, 9000 Ghent, Belgium.*

*2. DTU-Fotonik, Department of Photonics Engineering, Technical University of Denmark, Ørstedes Plads Building 343, 2800 Lyngby, Denmark.*

*3. Eindhoven University of Technology, Den Dolech 2, 5600 MB, Eindhoven, The Netherlands*

*4. Institut des Nanotechnologies de Lyon INL-UMR5270, CNRS, Université de Lyon, Ecole Centrale de Lyon, Ecully F-69134, France.*

*5. CEA, LETI, Minatec, 17 rue des Martyrs, 38054 Grenoble, France.*

*e-mail address: thijs.spuesens@intec.ugent.be*

**Abstract:** We demonstrate efficient photodetectors on top of a laser epitaxial structure completely fabricated using 200 mm wafer scale III-V/SOI technology enabling very dense integration of lasers and detectors for optical interconnect circuits.

**OCIS codes:** (040.5160) Photodetectors; (200.4650) Optical interconnects

## 1. Introduction

The increasing computer processing power puts stringent requirements on the bandwidth of interconnects. Current electrical interconnects are expected to soon reach their physical limits. Optical interconnects are believed to be a viable candidate to replace electrical interconnects for transporting large amounts of data between processor cores because of their huge bandwidth and additional flexibility through wavelength multiplexing schemes [1, 2]. Silicon-on-Insulator (SOI) is an interesting platform for such optical interconnects because it is compatible with CMOS fabrication technology and the high refractive index contrast allows for very compact integration. However, the intrinsic material properties of silicon make it very difficult to achieve active functionalities and therefore there is a lot of interest in integrating other materials with silicon. Two interesting approaches for photodetection are Ge-on-SOI and III-V-on-SOI. Germanium based photodetectors are fabricated by heteroepitaxial growth on silicon and have been demonstrated for wavelengths from 1.3 to 1.5  $\mu\text{m}$  [3, 4]. However, because of the lattice mismatch between silicon and germanium, special growth strategies are required and the absorption coefficient of Ge drops largely for wavelengths above 1.55  $\mu\text{m}$ . Additionally, for other active components, such as lasers and amplifiers, III-V semiconductors are the material of choice and these can be integrated on SOI by a molecular or adhesive bonding process [5, 6]. Several heterogeneously integrated lasers and detectors have already been demonstrated [7-9], but these require different epitaxial structures for lasers and detectors and therefore different III-V dies need to be bonded on the SOI. This limits the integration density because lasers and detectors need to be spatially separated to enable the bonding of the different III-V dies.

In this paper we report on III-V thin-film PIN photodetectors heterogeneously integrated on SOI using molecular die-to-wafer bonding. Besides the III-V heterostructure for these photodetectors, the bonded epitaxial structure also contains a III-V heterostructure for integrated lasers thereby enabling simultaneous and very dense integration of both lasers and photodetectors. Furthermore, all processing, including molecular bonding, III-V etching and metallization is performed in a 200 mm CMOS pilot line using 248 nm DUV lithography.

## 2. Design and fabrication

A schematic representation of the photodetector on top of the waveguide is shown in figure 1(a). An evanescent coupling scheme is used so that light from the underlying silicon waveguide with a height of 220 nm and width of 500 nm is coupled in the thin film detector on top of it. For efficient evanescent coupling the bonding layer thickness should be 100 to 200 nm thick. The fabricated devices have bonding layers thicknesses of  $\sim 130$  nm. The complete epitaxial structure consists of a detector heterostructure on top of a laser heterostructure and has a total thickness of  $\sim 1$   $\mu\text{m}$ . The epitaxial structure of the detector consists of a 400 nm thin i-InGaAs layer sandwiched between a 100 nm heavily doped p-type InGaAs top contact layer and an 80 nm n-type InP bottom contact layer which also serves as the top contact for the laser. Detector lengths vary from 20  $\mu\text{m}$  to 100  $\mu\text{m}$  and the mesa has a width of 3.5  $\mu\text{m}$ . In case a laser is required, the detector InGaAs layers are etched away so that a 580 nm structure remains. The laser epitaxial structure contains 3 compressively strained InAsP quantum wells and a tunnel junction. For a detailed description of the laser and its epitaxial structure we refer to [10]. Figure 1(b) shows a schematic representation of an optical interconnect with a laser and detector using a single epitaxial structure.

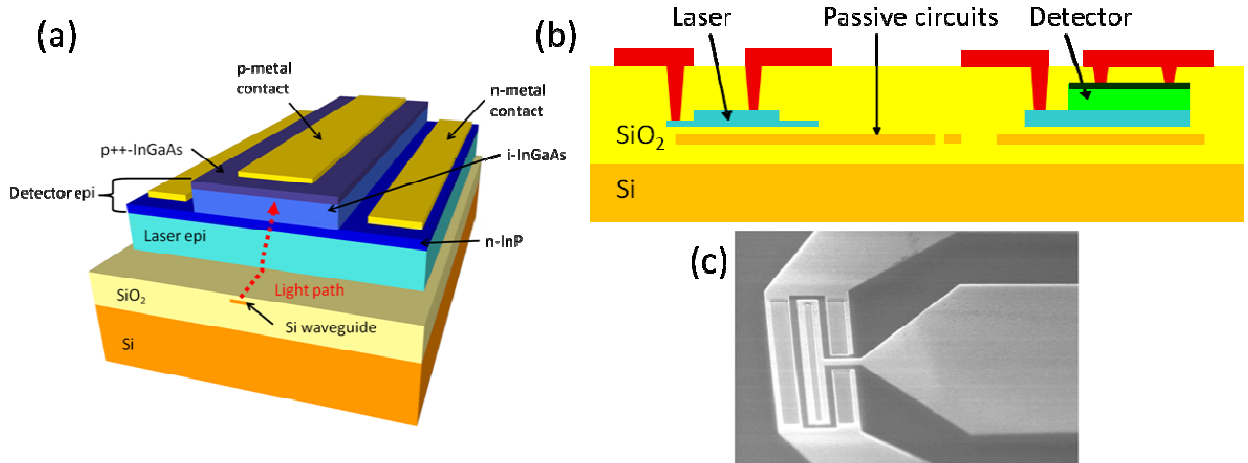


Fig. 1. (a) schematic representation of the detector structure. (b) optical interconnect cross section with a laser and detector from a single epi and (c) SEM picture of the fabricated detector.

The III-V die is molecularly bonded on top of the patterned SOI design after which the InP substrate is removed by a wet etching process. After substrate removal, the detector structure is subsequently patterned and etched using 248 nm deep ultraviolet (DUV) lithography and a wet etching process. A silicon oxide passivation layer is deposited and planarized using chemical-mechanical polishing (CMP). Vias, to reach both the top and bottom contact layers, are etched and a metal stack is full-sheet deposited. In order to have CMOS compatible contacts a Ti/TiN/AlCu metal stack is used instead of the normal gold-based contacts. A chlorine based chemistry is used to dry-etch the metal stack. A contact resistance of respectively  $1\text{e-}4\ \Omega.\text{cm}^2$  and  $6\text{e-}5\ \Omega.\text{cm}^2$  is obtained for  $5\text{e}18\text{cm}^{-3}$  n-InP and  $3\text{e}19\text{cm}^{-3}$  p-InGaAs [11]. Figure 1(c) shows a SEM picture of the fabricated detector.

### 3. Results and Discussion

The current-voltage (IV) characteristics with and without illumination were measured using a tunable laser source and a Keithley 2400 IV source/meter. Figure 2(a) shows the IV characteristics of both a 20 (red) and 80 (black)  $\mu\text{m}$  long detector. At a reverse bias of -2 V the measured dark current is  $1.9\ \mu\text{A}$  and  $7.9\ \mu\text{A}$  for a 20 and 80  $\mu\text{m}$  detector length, respectively. These dark current values are quite large for InGaAs based devices and are probably caused by not timely passivating the structure, resulting in a lot of surface states and therefore high surface recombination. By careful passivation the dark current is expected to reduce. For the IV measurement under illumination, light was coupled into the silicon waveguide via a grating coupler [12] at a wavelength of 1550 nm. The grating coupler efficiency was found to be maximum around 1584 nm with a value of 27 % and the efficiency at 1550 nm was 15 %. The light power was measured just before the grating coupler and was found to be 2.88 mW resulting in 432  $\mu\text{W}$  of power in the waveguide. This optical power generates a photocurrent of 310  $\mu\text{A}$  and 420  $\mu\text{A}$  for a 20  $\mu\text{m}$  and 80  $\mu\text{m}$  long photodetector, respectively. This corresponds with responsivities of 0.71 and 0.97 A/W. From the slopes of the IV curves under forward bias it was found that the series resistance is  $\sim 100\ \Omega$  for both devices.

The detected current was also measured versus the optical wavelength and the results are shown in figure 2(b). The dashed line shows the input power in the SOI waveguide and the solid line represents the detected current. The Gaussian shaped spectrum is caused by the grating coupler. One can see that the responsivity is more or less constant up to 1575 nm after which it starts to decrease slowly.

The frequency response of the detectors was measured with an Agilent N4373B Light Component Analyzer (LCA). First, a calibration procedure was executed to account for losses in the RF cables, RF probe and the bias-tee. Then, the modulated optical output from the LCA was coupled into the SOI waveguide via a grating coupler, while the electrical input from the LCA was connected to the detector via a bias-tee to measure electrical RF response. A Keithley 2000 IV meter was used to monitor the average photocurrent. Figure 3 shows the frequency response for both the detector structures. The 3dB bandwidth under a reverse bias of -1.5 V was around 9 GHz for the 80  $\mu\text{m}$  long detector and around 16 GHz for the detector with a length of 20  $\mu\text{m}$ . The lower bandwidth for the 80  $\mu\text{m}$  long detector can be explained by the larger capacitance following from an increased mesa area. From the measured series resistance and 3 dB bandwidth we find that the capacitance of the detector including the pads is in the order of

a few hundred fF. This is in good agreement with the calculated values for the parasitic capacitance of the detector which are 20 and 80 fF for the 20 and 80  $\mu\text{m}$  long detector, respectively.

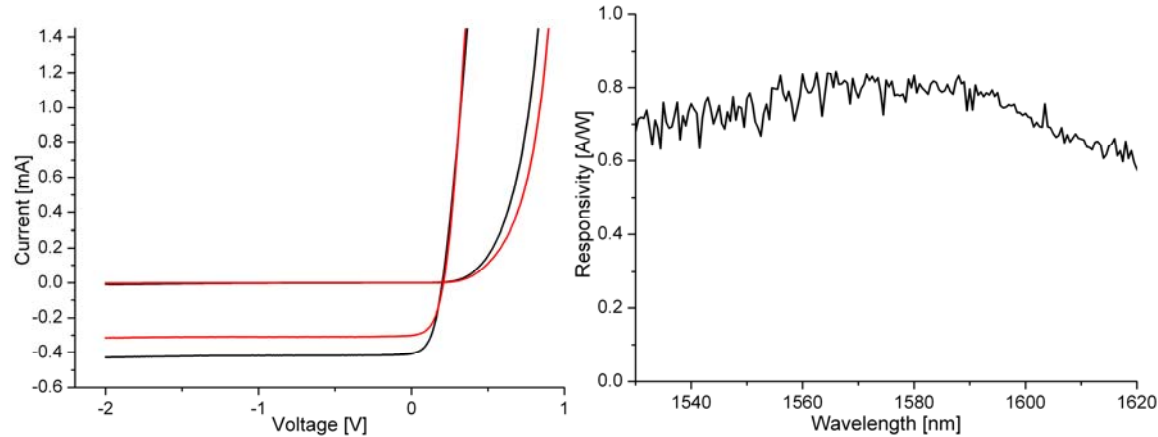


Fig. 2.(a) IV characteristic of a 20  $\mu\text{m}$  (red) and 80  $\mu\text{m}$  (black) long detector with and without illumination. (b) Responsivity versus wavelength for a 20  $\mu\text{m}$  long detector.

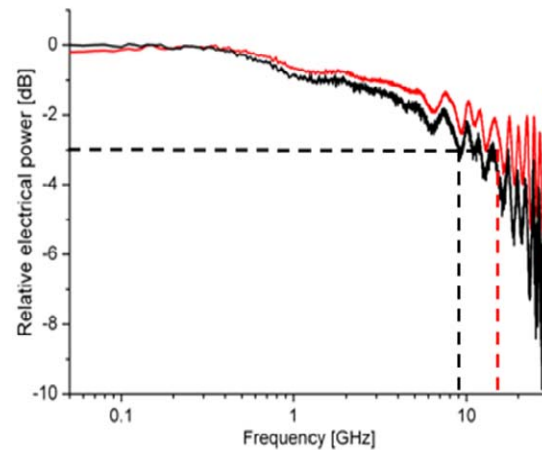


Fig. 3. Frequency response of a 20  $\mu\text{m}$  (red) and 80  $\mu\text{m}$  (black) long detector at a reverse bias of -1.5 V.

## Acknowledgment

This work was supported by the European FP7 ICT WADIMOS project. The work of T. Spuesens and D. Vermeulen is supported by the Institute for the Promotion of Innovation through Science and Technology (IWT) under a specialization grant.

## References

- [1] Haurylau, M., et al., *On-chip optical interconnect roadmap: Challenges and critical directions*. Selected Topics in Quantum Electronics, IEEE Journal of, 2007. **12**(6): p. 1699-1705.
- [2] Miller, D.A.B., *Rationale and challenges for optical interconnects to electronic chips*. Proceedings of the IEEE, 2002. **88**(6): p. 728-749.
- [3] Chen, L. and M. Lipson, *Ultra-low capacitance and high speed germanium photodetectors on silicon*. Optics Express, 2009. **17**(10): p. 7901-7906.
- [4] Vivien, L., et al., *42 GHz pin Germanium photodetector integrated in a silicon-on-insulator waveguide*. Optics Express, 2009. **17**(8): p. 6252-6257.
- [5] Roelkens, G., et al., *Adhesive Bonding of InP/ InGaAsP Dies to Processed Silicon-On-Insulator Wafers using DVS-bis-Benzocyclobutene*. Journal of the Electrochemical Society, 2006. **153**: p. G1015.
- [6] Kostrzewa, M., et al. *Die-to-wafer molecular bonding for optical interconnects and packaging*.
- [7] Binetti, P.R.A., et al. *InP/InGaAs photodetector on SOI circuitry*. 2009.
- [8] Fang, A.W., et al., *Electrically pumped hybrid AlGaInAs-silicon evanescent laser*. Optics Express, 2006. **14**(20): p. 9203-9210.
- [9] Sheng, Z., et al., *InGaAs PIN photodetectors integrated on silicon-on-insulator waveguides*. Optics Express. **18**(2): p. 1756-1761.
- [10] Spuesens, T., et al. *Improved design of an InP-based microdisk laser heterogeneously integrated with SOI*. Group IV Photonics 2009, 2009.
- [11] Grenouillet, L., et al., *CMOS compatible contacts and etching for InP-on-silicon active devices*. Group IV Photonics 2009, 2009.
- [12] Taillaert, D., et al., *An out-of-plane grating coupler for efficient butt-coupling between compact planar waveguides and single-mode fibers*. Quantum Electronics, IEEE Journal of, 2002. **38**(7): p. 949-955.